Engineered Science
DOI: https://dx.doi.org/10.30919/es1514

# Evaluating Failure Patterns and Bursting Loads in Concrete Segmental Bridge Piers: A Comprehensive Study

Suniti Suparp,[1, 2] Ali Ejaz,[3] Chaitanya Krishna Gadagamma,[4, 5] Panumas Saingam,[6] Qudeer Hussain,[7,*] Panuwat Joyklad,[1, 2] Preeda Chaimahawan,[8,*] Gritsada Sua-Iam,[9] Burachat Chatveera[10] and Mohammad Noor Jan Ahmadi[11]

## Abstract

This study presented an experimental and numerical investigation focused on pier segments of segmental bridge types. The pier segments were constructed to represent Lak Si Overpass Highway Route No. 304, Thailand. The experimental program included five pier segments with similar reinforcement details but varying concrete strengths. The numerical work validated the finite element model (FEM) using experimental results and conducted a parametric study to assess the impact of steel reinforcement variation and concrete compressive strength on the bursting capacity of pier segments. Key findings included a consistent failure pattern characterized by a prominent vertical crack and concrete crushing at the bottom, particularly in specimens with lower concrete strength. The bursting loads exhibited a decrease corresponding to a reduction in compressive strength, with up to a 20% decrease observed when strength was reduced by 20%. The finite element analysis (FEA) results slightly surpassed experimental findings, yet the marginal discrepancies confirmed the accuracy of the advanced tool for engineering nonlinear analysis (ATENA) computer program in predicting bursting forces. The parametric study highlighted a substantial increase in bursting loads with variations in concrete strength and the number of steel reinforcement layers, with a non-proportional relationship between bursting load and concrete strength.

*Keywords:* Pier segments; Compressive strength; Steel reinforcement ratio; Bursting load; Finite element modeling; Advanced tool for engineering nonlinear analysis.
Received: 02 December 2024; Revised: 25 February 2025; Accepted: 06 March 2025.
Article type: Research article.

## 1. Introduction

Precast, pre-stressed concrete box girders find extensive application in short- and medium-span bridges globally.[1] The prevalent configuration for box girder bridges involves the combination of individual box sections.[2] Since their inception in the 1950s, adjacent precast box girder bridges have consistently demonstrated robust performance.[3] The development, global adoption, and straightforward principles of segmental construction in the domain of post-tensioned concrete segmental bridges stand as one of the most captivating accomplishments in the field of bridge engineering.[4–6] Moreover, conventional box girder systems present an aesthetically pleasing and structurally viable solution for bridging infrastructures in expansive urban environments.[7–9] A precast, pre-stressed concrete box girder bridge consists of end segments, typical segments, deviator segments, tendons, anchors, and joints. Construction begins with placing the end segments on pier columns, followed by installing the typical and deviator segments using different methods.[10,11]

Significant research has focused on the performance of precast, pre-stressed concrete box girder bridges. Yuan *et al*. studied segmental concrete box beams with internal and external tendons under bending. Their experiments on three scaled specimens with varying tendon ratios revealed important effects on load-carrying capacity, ductility, and failure mode.[12] Jiang *et al*.[13] conducted an analysis on the flexural behavior of precast concrete segmental beams

[1] *Department of Civil and Environmental Engineering, Faculty of Engineering, Srinakharinwirot University, Nakhonnayok, 26120, Thailand*
[2] *Center of Excellence in Rail System Technology and Civil Engineering Material Innovation for Sustainable Infrastructure, Strategic Wisdom and Research Institute, Srinakharinwirot University, Bangkok, 10110, Thailand*
[3] *National Institute of Transportation, National University of Sciences and Technology (NUST), Islamabad, 44000, Pakistan*
[4] *Structural Engineering, School of Engineering and Technology, Asian Institute of Technology (AIT), Klong Luang, 12120, Thailand*
[5] *Department of Civil Engineering, Chennai Institute of Technology, Chennai, 600069, India*

incorporating hybrid tendons and dry joints. Tests showed that these beams exhibited satisfactory flexural capacity and enhanced ductility. Investigating shear behavior in precast concrete segmental box girder bridges, Ahmed *et al*.[14] tested single-cell specimens with dry and epoxied joints under direct shear loading. Results revealed that epoxy minimizes joint imperfections, ensuring uniform shear stress distribution. Fully post-tensioned epoxied joints exhibited perfect closure and shear transfer upon immediate application. Chai *et al*.[15] examined the long-term performance of precast concrete segmental box girders with dry joints through an extensive one-year laboratory study. They found that factors such as shorter concrete age at loading, lower concrete strength, fewer segments, smaller reinforcement ratio, more shear keys, higher initial pre-stress, and greater external load led to significant structural deterioration, including pre-stress loss and increased deflection.

Zhou *et al*.[16] conducted a transverse analysis on full-scale precast segmental box girder segments with corrugated steel webs. The results showed that bending failure of the top concrete flange occurred before shear buckling of the corrugated steel webs. The performance of an unbounded post-tensioned concrete pier segment can be influenced by factors including concrete strength, tendon reinforcement ratio, and the applied post-tensioning force.[17–19] Wu *et al*.[20] conducted nonlinear finite element analysis (FEA) on bridge pier segments, studying concrete strengths ranging from 30 MPa to 75 MPa. They found that while changes in concrete strength did not affect the failure mode, the extent of damage decreased as the concrete strength increased. Zhang and Alam performed FEA on bridge segment piers and varied the tendon force and concrete strength.[21] The yielding base shear was found to increase with the increase in compressive strength. A higher concrete strength enhanced the pier's compressive resistance and stiffness, leading to a delayed reduction in post-elastic stiffness. He *et al*.[22] introduced a crack-based methodology for evaluating the serviceability performance of cracked box-girders. Their investigation revealed a correlation between crack width and crack spacing, which, in turn, was associated with the compressive strength of the concrete.

To date, experimental studies on the performance of box girder pier segments have been limited in their examination of varying concrete strength and longitudinal reinforcement ratio.

Previous investigations have not extensively addressed these factors and have predominantly relied on FEA to examine these effects.[15,16,20,23] Some other studies have reported the use of theoretical equations and FEA for concrete members.[24,25] This study endeavors to address this research gap through a comprehensive experimental campaign involving five pier segments, each characterized by distinct concrete strengths and variations in longitudinal reinforcement ratios. Additionally, finite element modeling, implemented through the advanced tool for engineering nonlinear analysis (ATENA) software,[26] was employed to replicate and augment the observed behavior of the pier segments. It is important to note that bridge pier end segments were utilized in this study by fabricating their scaled-down version.

## 2. Experimental program

### 2.1 Test matrix

In this study, five reduced-scale pier segments were tested. The pier segments were constructed to represent the Lak Si Overpass Highway Route No. 304, Thailand. The highway route No. 304 is a national highway, which connects Bangkok to Nakhon Ratchasima in the country's Northeast. A constructed part of highway route No. 304 is shown in Fig. 1(a). The pier segments were reduced to 1/4$^{th}$ scale, and specimens were distinguished by the strength of their concrete. Details of specimens are given in Table 1, which is listed in decreasing order of their compressive strengths. A two-part terminology was used to identify specimens. The first part, *i.e.*, ES, designated the specimen type that is the end segment. Whereas the second part denoted the concrete strength in MPa. For instance, ES-30 denoted an end segment constructed with a 30 MPa concrete strength. The total height of the pier segment was 500 mm, whereas the top and bottom widths were 1200 mm and 1000 mm, respectively, as shown in Fig. 1(a). An opening of 230 mm by 250 mm in height and width, respectively, was provided, as depicted in Fig. 1(c).

### 2.2 Material properties

Type-1 Portland cement constituted the primary binder in the concrete mix for all specimens. Fine aggregates sourced from locally available river sand were utilized. The coarse aggregates adhered to a maximum size constraint of 25 mm. The compressive strength of all segments was evaluated by casting cylinders as per the recommendations of ASTM C1314-23a.[27] The measured compressive strengths were 40 MPa, 35 MPa, 30 MPa, 25 MPa, and 20 MPa for specimens ES-40, ES-35, ES-30, ES-25, and ES-20, respectively. The longitudinal reinforcement consisted of 25 mm-diameter

[6] *Department of Civil Engineering, King Mongkut's Institute of Technology Ladkrabang, Bangkok, 10520, Thailand*
[7] *Civil Engineering Department, Kasem Bundit University, Bangkok, 10250, Thailand*
[8] *School of Engineering, University of Phayao, Phayao, 56000, Thailand*
[9] *Department of Civil Engineering, Faculty of Engineering, Rajamangala University of Technology Phra Nakhon, Bangkok, 10800, Thailand*
[10] *Department of Civil Engineering, Faculty of Engineering, Thammasat University (Rangsit Campus), Pathum Thani, 12121, Thailand*
[11] *Civil Department, Engineering Faculty, Shaikh Zayed University, Khost, 2553, Afghanistan*
**Email:* ebbadat@hotmail.com (Q. Hussain); preeda.ch@up.ac.th (P. Chaimahawan)

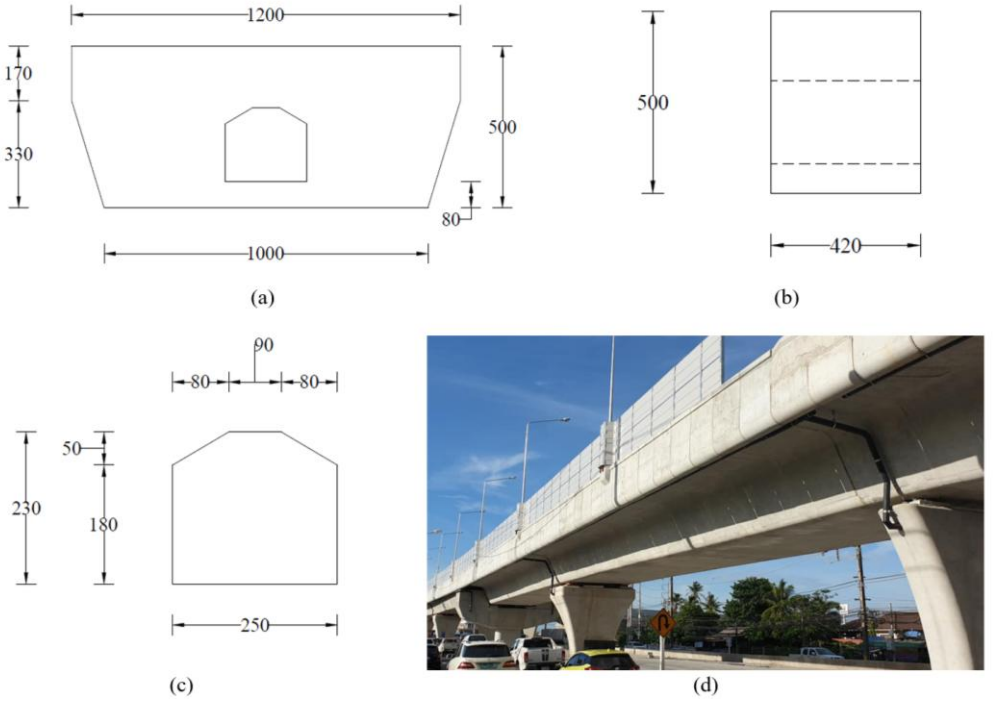


**Fig. 1:** Typical specimen geometry (a) front elevation of tested segment, (b) side view, (c) opening details and (d) typical construction of highway route No. 304 (units in mm).

deformed bars, whereas stirrups consisted of 16 mm deformed bars placed at 100 mm center to center. The mechanical properties of steel bars were obtained by following the protocols of ASTM E8/E8M-21.[28] The yield and ultimate strength of longitudinal bars were 500 MPa and 640 MPa, respectively. Whereas the yield and ultimate strength of transverse bars were 400 MPa and 450 MPa, respectively.

**Table 1:** Details of specimens.

| Pier segment | Mix type | Concrete strength (MPa) |
|---|---|---|
| ES-40 | Type-1 | 40 |
| ES-35 | Type-2 | 35 |
| ES-30 | Type-3 | 30 |
| ES-25 | Type-4 | 25 |
| ES-20 | Type-5 | 20 |

### 2.3 Construction process

Wooden formwork molds were designed to match the required dimensions of segments. After placing the necessary reinforcement, concrete was mixed and poured into the molds, ensuring proper compaction. The steel cage was prepared outside of the mold. After placing spacers on all sides of molds, steel cages were inserted into the molds. It is noteworthy that the open spaces inside segments were incorporated by erecting wooden sheets in the necessitated shape and dimensions. A typical formwork before concrete pouring is shown in Fig. S1. After one day of casting, the formworks were removed and left for curing for a period of 28 days. A typical pier segment after curing period is shown in Fig. S2.

### 2.4 Test setup and instrumentation

To examine the bursting forces in the anchorage zone of precast lightweight concrete segments for segmental box girder bridges, individual end segments underwent pure axial

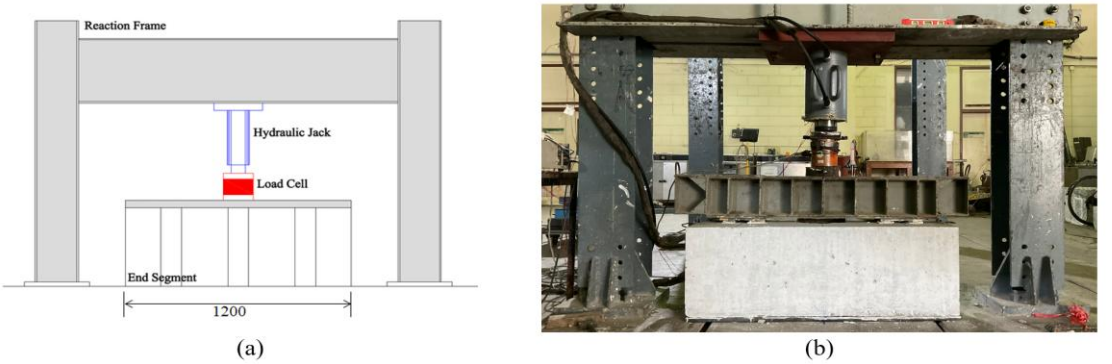


**Fig. 2:** Test setup: (a) schematics and (b) actual setup (units in mm).

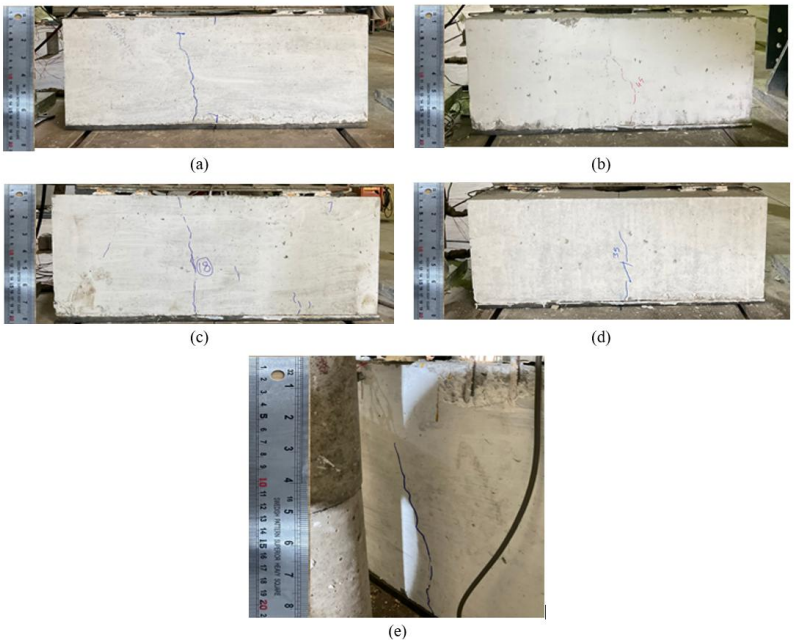


**Fig. 3:** Failure mode of specimen: (a) ES-40, (b) ES-35, (c) ES-30, (d) ES-25, and (e) ES-20.

compression testing. The load was applied along the longitudinal axis of the end segments, which were rotated and positioned on a rigid surface. A specially designed loading frame was constructed to facilitate the testing of the proposed end segments. The typical test setup is displayed in Fig. 2. The load was imposed through a hydraulic jack affixed to the top beam of the frame, with the magnitude of the imposed load being estimated by a load cell positioned directly beneath the hydraulic jack.

## 3. Experimental results

### 3.1 Failure modes

Notably, the failure of all specimens did not accompany several cracks. However, a major vertical crack was observed in all specimens, as shown in Fig. 3. This crack initiated at the bottom and traversed towards the top as the loading progressed. Concrete crushing at the bottom was also observed for specimens with low concrete strength, as presented in Fig. S3.

### 3.2 Bursting loads

The bursting forces of end segments in the form of ultimate load recorded at the load cell are summarized in Table 2. The bursting forces of end segments decreased as the concrete strength decreased. The bursting forces were reduced by 5%, 8%, 14% and 20% for end segments ES-35, ES-30, ES-25, and ES-20, respectively. when compared with Specimen ES-40. Fig. 4 shows this variation in ultimate load and comparison with that of Specimen ES-40.

**Table 2:** Bursting forces of all specimens and percentage reduction with concrete strength.

| Pier segment | Ultimate load (kN) | Reduction in ultimate load (%) |
|---|---|---|
| ES-40 | 95.00 | - |
| ES-35 | 90.00 | 5 |
| ES-30 | 87.00 | 8 |
| ES-25 | 82.00 | 14 |
| ES-20 | 76.00 | 20 |

### 3.3 Finite element modeling

The structural behavior of the pier segment was assessed

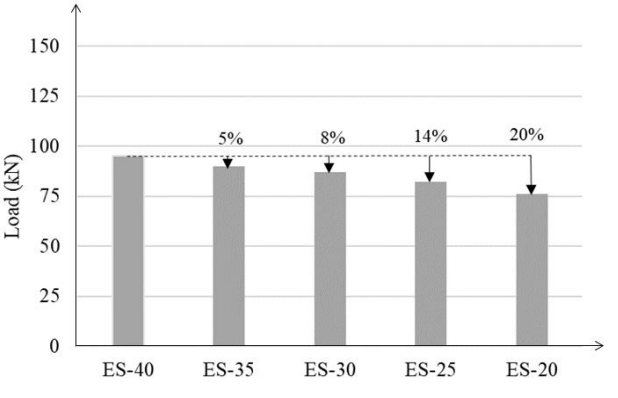


**Fig. 4:** Variation in ultimate load of segments and comparison with that of Specimen ES-40.

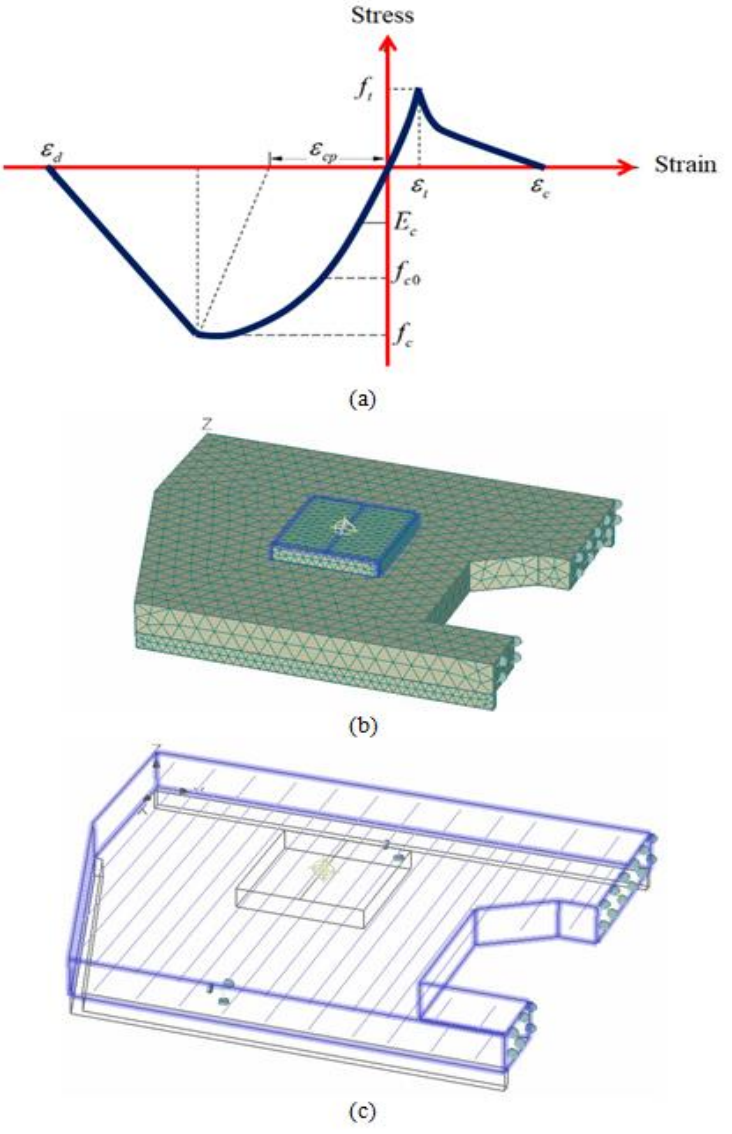


**Fig. 5:** Modeling details: (a) Uniaxial stress vs strain relation for concrete adopted by ATENA ,[26,30] (b) ATENA FEM modeling after mesh generation, and (c) Reinforcement details in FEM modeling.

utilizing ATENA, a specialized software for concrete structures,[26,29] renowned for its user-friendly interface, integrated material models, and effective convergence solutions.[30,31] ATENA's capabilities extend to the realistic analysis of bridge structures.[26,27]

### 3.4 Modeling details

In this study, the pier segment was evaluated utilizing the material models for steel, concrete, and other relevant materials. In this model, 1D truss elements were employed to represent the reinforcement bars, and their material properties were defined by means of the CCReinforcement material model, also existing in ATENA. The multi-linear choice for steel was chosen to incorporate plastic hardening. ATENA works on the assumption of a perfect bond between steel and concrete. All reinforcement bars were assumed to have a perfect bond with the concrete elements. The stress-strain relationship for the reinforcement bars was modeled using a multi-linear plastic model. Constitutive law 'CC3DNonLinCementitious2' was used to model concrete. The uniaxial stress (σ) vs. strain (Ɛ) relation of concrete adopted by ATENA is shown in Fig. 5(a). The mesh size was kept at 50 mm, making a total of 12463 elements in the domain. A typical element after mesh generation is revealed in Fig. 5(b). The reinforcement details are displayed in Fig. 5(c).

### 3.5 Comparison of bursting loads

The finite element analysis in terms of ultimate loads (bursting forces) of end segments is summarized in Table 3 along with experimental results. The finite element analysis results were slightly higher than the experimental results. However, the differences were small, and it can be concluded that the computer program ATENA is well capable of accurately predicting the bursting forces of the end segments. Moreover, the percentage difference between experimental and predicted loads was restricted below 7%, as shown in Table 3.

**Table 3:** Comparison of experimental and predicted bursting loads.

| Pier segment | Ultimate Load (kN) | | Difference (%) |
|---|---|---|---|
| | FEM | Experimental | |
| ES-40 | 101.00 | 95.00 | 6.32 |
| ES-35 | 96.00 | 90.00 | 6.66 |
| ES-30 | 93.00 | 87.00 | 6.89 |
| ES-25 | 87.00 | 82.00 | 6.10 |
| ES-20 | 80.00 | 76.00 | 5.26 |

**Table 4:** Details of FEM models for parametric study.

| No. | Concrete Strength (MPa) | Spacing of Steel Bars (mm) | Layers of Steel Bars | Ultimate Load (kN) |
|---|---|---|---|---|
| 1 | 25 | 0 | 0 | 276 |
| 2 | 25 | 200 | 1 | 359 |
| 3 | 25 | 200 | 2 | 374 |
| 4 | 25 | 100 | 1 | 413 |
| 5 | 25 | 100 | 2 | 432 |
| 6 | 50 | 0 | 0 | 382 |
| 7 | 50 | 200 | 1 | 526.6 |
| 8 | 50 | 200 | 2 | 534.5 |
| 9 | 50 | 100 | 1 | 614.6 |
| 10 | 50 | 100 | 2 | 622.9 |
| 11 | 100 | 0 | 0 | 550.5 |
| 12 | 100 | 200 | 1 | 691.9 |
| 13 | 100 | 200 | 2 | 723.1 |
| 14 | 100 | 100 | 1 | 873.3 |
| 15 | 100 | 100 | 2 | 911.5 |

### 3.6 Parametric study

The FEM model was further extended to study the behavior of pier segment by modifying the steel reinforcement. The concrete strength was varied as 25 MPa, 50 MPa, and 100 MPa. For each concrete strength, five FEM models were prepared. One model did not incorporate steel reinforcement. Two models incorporated steel reinforcement placed at 200 mm and 100 mm. For each spacing of steel reinforcement, one or two layers of steel reinforcement were considered. Table 4 presents the details of FEM models considered in this parametric study.

Fig. S4 depicts the cracking patterns and stress distribution in specimens with a concrete strength of 25 MPa, whereas cracking patterns for 50 MPa and 100 MPa concrete strength are given in Figs. S5 and S6, respectively. The control specimens experienced the greatest stresses in concrete because of the absence of steel reinforcement. This can be observed from the bottom views of control specimens as demonstrated by stresses in red color. Crack patterns, in general, were similar in all specimens, irrespective of the magnitude of the concrete strength or steel reinforcement. However, the bursting loads varied significantly with concrete strength and steel reinforcement. In particular, a significant increase in bursting loads was observed by changing the concrete strength or the number of layers of steel reinforcement. For instance, specimens 2, 7, and 12 were constructed with concrete strengths of 25 MPa, 50 MPa, and 100 MPa, respectively, and contained a single layer of steel reinforcement at 200 mm spacing. The corresponding bursting loads were observed at 359 kN, 526.6 kN, and 691.9 kN, respectively. This corresponds to an increase of 46.6% and 92.7% when the compressive strength was increased by 100% and 300%, respectively. This suggests that the increase in bursting load is not proportional to the concrete strength. Nonetheless, a significant increase in bursting load suggests a substantial dependence of the bursting load on the compressive strength of the segment pier.

The load vs. deflection curves are shown in Figs. 6(a)-(c) for specimens with 25 MPa, 50 MPa, and 100 MPa concrete strength, respectively. It can be observed that steel reinforcement substantially improved the ductility. It is observed that increasing the layers does not significantly contribute to the bursting load. However, reducing the spacing of steel reinforcements from 200 mm to 100 mm enhanced the bursting capacity significantly. Another important observation is that doubling the layers of steel reinforcement can negatively affect the ductility of pier segments.

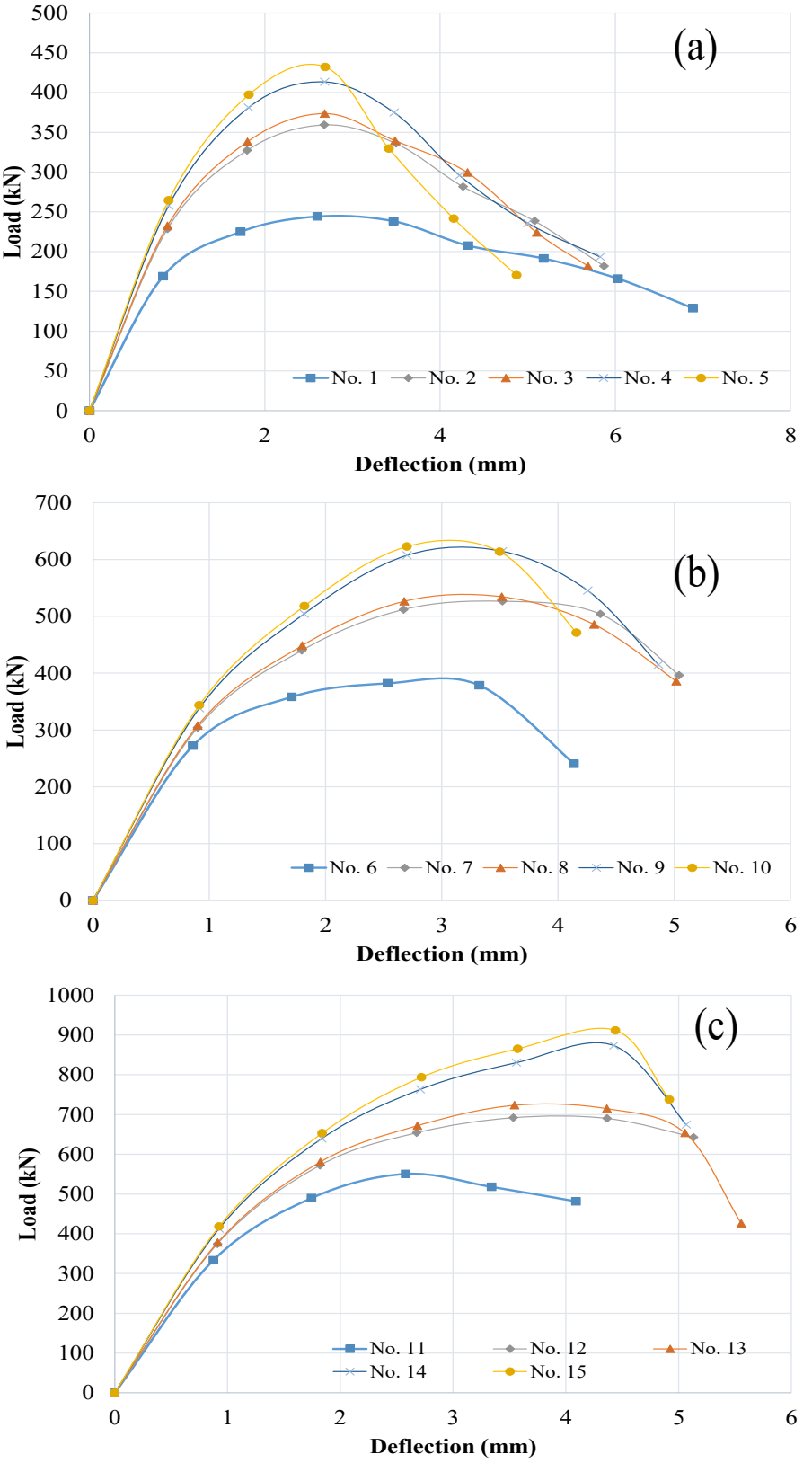


**Fig. 6:** Load vs. deflection curves of pier segments with concrete strength of: (a) 25 MPa, (b) 50 MPa, and (c) 100 MPa.

## 4. Conclusion

This study presented an experimental and numerical work on pier segments of segmental bridge types. The experimental program comprised five pier segments having similar reinforcement details but different concrete strengths. The numerical work first validated the FEM model from experimental results. Then, a parametric study on the validated model was conducted to determine the effect of the variation in steel reinforcement and compressive strength of concrete on the bursting capacity of pier segments. The following

conclusions were drawn from this work.

Significantly, the failure of all specimens did not involve multiple cracks; rather, a prominent vertical crack was evident in each specimen. Additionally, concrete crushing at the bottom was observed in specimens with lower concrete strength. In general, the failure pattern did not vary significantly, which might be related to the fact that concrete strength did not vary significantly in experimental work. The bursting loads exhibited a decline as the compressive strength of the concrete decreased. A 20% reduction in compressive strength resulted in a corresponding drop in bursting load by up to 20%. The results of the finite element analysis were marginally higher than the experimental findings. Nonetheless, the discrepancies were minor, leading to the conclusion that the computer program ATENA is adept at accurately forecasting the bursting forces of the end segments. Furthermore, the percentage difference between experimental and predicted loads remained below 7%.

The parametric study revealed a noteworthy increase in bursting loads with variations in concrete strength and the number of layers of steel reinforcement. For example, specimens 2, 7, and 12, constructed with concrete strengths of 25 MPa, 50 MPa, and 100 MPa, respectively, and featuring a single layer of steel reinforcement at 200 mm spacing, exhibited bursting loads of 359 kN, 526.6 kN, and 691.9 kN, respectively. This signifies an increase of 46.6% and 92.7% when the compressive strength was elevated by 100% and 300%, respectively. The findings suggest that the increase in bursting load is not directly proportional to the concrete strength. Nevertheless, the substantial rise in bursting load underscores a notable dependency on the compressive strength of the segment pier.

Load vs. deflection curves obtained from the parametric study indicated a substantial enhancement in ductility with the inclusion of steel reinforcement. The analysis revealed that increasing the layers of reinforcement did not notably contribute to the bursting load. Conversely, a significant improvement in bursting capacity was observed when reducing the spacing of steel reinforcements from 200 mm to 100 mm. Additionally, a noteworthy observation was that doubling the layers of steel reinforcement could have a detrimental impact on the ductility of pier segments.

**Acknowledgement**

This study Received Research Funding from Faculty of Engineering's (Srinakharinwirot University, Thailand) income for Fiscal Year 2024, (Contract No. 204/2567). Thanks are also extended to Asian Institute of Technology (AIT), Thailand for supporting test facilities.

**Conflict of Interest**

There is no conflict of interest.

**Supporting Information**

Applicable.

**References**

[1] K. Hu, X. Shi, X. Ruan, C. Liang, Z. Liu, The second Wuhu bridge: an industrialized application of external pre-stressed box-girder bridge in China, *Structural Engineering International*, 2017, **27**, 315-320, doi: 10.2749/101686617x14881932436375.

[2] K. M. Sennah, J. B. Kennedy, Literature review in analysis of box-girder bridges, *Journal of Bridge Engineering*, 2002, **7**, 134-143, doi: 10.1061/(asce)1084-0702(2002)7:2(134).

[3] D. Y. Moon, J. Sim, H. Oh, Practical crack control during the construction of precast segmental box girder bridges, *Computers & Structures*, 2005, **83**, 2584-2593, doi: 10.1016/j.compstruc.2005.05.001.

[4] G. H. Ahmed, O. Q. Aziz, Influence of intensity & eccentricity of posttensioning force and concrete strength on shear behavior of epoxied joints in segmental box girder bridges, *Construction and Building Materials*, 2019, **197**, 117-129, doi: 10.1016/j.conbuildmat.2018.11.220.

[5] M. Usman, M. Yaqub, M. Auzair, W. Khaliq, M. Noman, A. Afaq, Restorability of strength and stiffness of fire damaged concrete using various composite confinement techniques, *Construction and Building Materials*, 2021, **272**, 121984, doi: 10.1016/j.conbuildmat.2020.121984.

[6] S. Ahmad, A. Shah, A. Nawaz, K. Salimullah, Shear strengthening of corbels with carbon fibre reinforced polymers (CFRP), *Materiales de Construcción*, 2010, **60**, 79-97, doi: 10.3989/mc.2010.50009.

[7] G. H. Ahmed, O. Q. Aziz, Stresses, deformations and damages of various joints in precast concrete segmental box girder bridges subjected to direct shear loading, *Engineering Structures*, 2020, **206**, 110151, doi: 10.1016/j.engstruct.2019.110151.

[8] Q. Li, L. Ibrahim, W. Zhou, M. Zhang, Z. Yuan, Treatment methods for plant fibers for use as reinforcement in cement-based materials, *Cellulose*, 2021, **28**, 5257-5268, doi: 10.1007/s10570-021-03903-w.

[9] A. Husnain, I. A. Qazi, W. Khaliq, M. Arshad, Immobilization in cement mortar of chromium removed from water using titania nanoparticles, *Journal of Environmental Management*, 2016, **172**, 10-17, doi: 10.1016/j.jenvman.2016.02.026.

[10] Z. Zhao, W. He, S. C. Fan, Preliminary design system for concrete box girder bridges, *Journal of Computing in Civil Engineering*, 2001, **15**, 184-192, doi: 10.1061/(asce)0887-3801(2001)15:3(184).

[11] K. Rodsin, P. Joyklad, Q. Hussain, H. Mohamad, A. Buatik, M. Zhou, K. Chaiyasarn, A. Nawaz, T. Mehmood, A. Elnemr, Behavior of steel clamp confined brick aggregate concrete circular columns subjected to axial compression, *Case Studies in Construction Materials*, 2022, **16**, e00815, doi: 10.1016/j.cscm.2021.e00815.

[12] A. Yuan, H. Dai, D. Sun, J. Cai, Behaviors of segmental concrete box beams with internal tendons and external tendons under bending, *Engineering Structures*, 2013, **48**, 623-634, doi: 10.1016/j.engstruct.2012.09.005.

[13] H. Jiang, Q. Cao, A. Liu, T. Wang, Y. Qiu, Flexural behavior of precast concrete segmental beams with hybrid tendons and dry joints, *Construction and Building Materials*, 2016, **110**, 1-7, doi:

10.1016/j.conbuildmat.2016.02.003.
[14] G. H. Ahmed, O. Q. Aziz, Shear behavior of dry and epoxied joints in precast concrete segmental box girder bridges under direct shear loading, *Engineering Structures*, 2019, **182**, 89-100, doi: 10.1016/j.engstruct.2018.12.070.
[15] S. Chai, T. Guo, Z. Chen, J. Yang, Monitoring and simulation of long-term performance of precast concrete segmental box girders with dry joints, *Journal of Bridge Engineering*, 2019, **24**, 04019043, doi: 10.1061/(asce)be.1943-5592.0001409.
[16] M. Zhou, Y. Liu, W. Deng, M. F. Hassanein, H. Zhang, Transverse analysis of full-scale precast segmental box girder segments with corrugated steel webs: Experimental tests and FE modelling, *Engineering Structures*, 2019, **187**, 231-241, doi: 10.1016/j.engstruct.2019.02.072.
[17] H. M. Dawood, M. ElGawady, Performance-based seismic design of unbonded precast post-tensioned concrete filled GFRP tube piers, *Composites Part B: Engineering*, 2013, **44**, 357-367, doi: 10.1016/j.compositesb.2012.04.065.
[18] H. Dawood, M. ElGawady, J. Hewes, Behavior of segmental precast posttensioned bridge piers under lateral loads, *Journal of Bridge Engineering*, 2012, **17**, 735-746, doi: 10.1061/(asce)be.1943-5592.0000252.
[19] P. Joyklad, A. Nawaz, Q. Hussain, Effect of fired clay brick aggregates on mechanical properties of concrete, *Suranaree Journal of Science and Technology*, 2018, **25**, 349-362.
[20] M. Wu, L. Jin, X. Du, Dynamic response analysis of bridge precast segment piers under vehicle collision, *Engineering Failure Analysis*, 2021, **124**, 105363, doi: 10.1016/j.engfailanal.2021.105363.
[21] Q. Zhang, M. S. Alam, Evaluating the seismic behavior of segmental unbounded posttensioned concrete bridge piers using factorial analysis, *Journal of Bridge Engineering*, 2016, **21**, 04015073, doi: 10.1061/(asce)be.1943-5592.0000851.
[22] Z. He, Y. Li, T. Xu, Z. Liu, Z. J. Ma, Crack-based serviceability assessment of post-tensioned segmental concrete box-girder bridges, *Structures*, 2021, **30**, 1097-1108, doi: 10.1016/j.istruc.2021.01.062.
[23] S. Farhan Mushtaq, A. Ali, R. A. Khushnood, R. F. Tufail, A. Majdi, A. Nawaz, S. Durdyev, D. D. Burduhos Nergis, J. Ahmad, Effect of bentonite as partial replacement of cement on residual properties of concrete exposed to elevated temperatures, *Sustainability*, 2022, **14**, 11580, doi: 10.3390/su141811580.
[24] S. Issa, A. Ashteyat, M. Abdel-Jaber, Shear strengthening and repairing of reinforced concrete T-beam exposed to high temperature using near surface mounted carbon fiber (NSM-CFRP) ropes, *Engineered Science*, 2024, **31**, 872, doi: 10.30919/es8d872.
[25] M. D. Sreeja, N. Nalanth, Exploring environmentally sustainable concrete: an analytical investigation on high performance concrete using cellulose nanofibers, *ES Energy & Environment*, 2025, **27**, 1382, doi: 10.30919/esee1382.
[26] V. Cervenka, J. Cervenka, R. Pukl, ATENA: a tool for engineering analysis of fracture in concrete, *Sadhana*, 2002, **27**, 485-492, doi: 10.1007/BF02706996.
[27] ASTM C1314-23a, Standard Test Method for Compressive Strength of Masonry Prisms, ASTM International, West Conshohocken, PE, USA, 2023.
[28] ASTM E8/E8M-21, Standard Test Methods for Tension Testing of Metallic Materials, ASTM International, West Conshohocken, PE, USA, 2021.
[29] A. F. A. de Mello, R. A. de Souza, Analysis and design of reinforced concrete deep beams by a manual approach of stringer-panel method, *Latin American Journal of Solids and Structures*, 2016, **13**, 1126-1151, doi: 10.1590/1679-78252623.
[30] P. Chaimahawan, S. Suparp, P. Joyklad, Q. Hussain, Finite element analysis of reinforced concrete pile cap using ATENA, *Latin American Journal of Solids and Structures*, 2021, **18**, 342, doi: 10.1590/1679-78256290.
[31] P. Kannam, V. R. Sarella, A study on validation of shear behaviour of steel fibrous SCC based on numerical modelling (ATENA), *Journal of Building Engineering*, 2018, **19**, 69-79, doi: 10.1016/j.jobe.2018.05.003.